VIP ***The following Communications have been judged by at least two referees to be "very important papers" and will be published online at www.angewandte.org soon:***

*Q. Zhang, T. P. Chou, B. Russo, S. A. Jenekhe, G. Cao**
Aggregation of ZnO Nanocrystallites for High Conversion Efficiency in Dye-Sensitized Solar Cells

*S. Arita, T. Koike, Y. Kayaki, T. Ikariya**
Aerobic Oxidative Kinetic Resolution of Racemic Secondary Alcohols with Chiral Bifunctional Amido Complexes

*C. Ruspic, J. R. Moss, M. Schürmann, S. Harder**
Remarkable Stability of Metallocenes with Superbulky Ligands: Spontaneous Reduction of Sm^{III} to Sm^{II}

T. A. Rokob, A. Hamza, A. Stirling, T. Soós, I. Pápai**
Turning Frustration into Bond Activation: A Theoretical Mechanistic Study on Heterolytic Hydrogen Splitting by Frustrated Lewis Pairs

*L. M. Fidalgo, G. Whyte, D. Bratton, C. F. Kaminski, C. Abell, W. T. S. Huck**
From Microdroplets to Microfluidics: Selective Emulsion Separation in Microfluidic Devices

News

New Members of the International Advisory Board: G. R. Desiraju, D. Gatteschi, K. Kim, S. G. Withers ——— 2728

Books

Modern Alkaloids — Ernesto Fattorusso, Orazio Taglialatela-Scafati — *reviewed by P. Spiteller* ——— 2730

Name Reactions for Functional Group Transformations — Jie Jack Li — *reviewed by D. Sälinger* ——— 2731

Highlights

Carbanion Arylations

P. O'Brien,* J. L. Bilke ——— 2734 – 2736

Expanding the Synthetic Potential of Asymmetric Deprotonation: Arylation of Carbanions

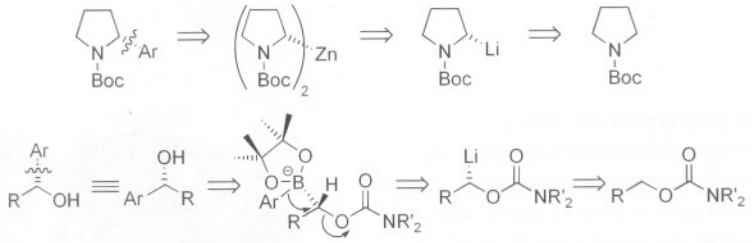

Aryl unplugged: Two conceptually new disconnections are equivalent to arylation of enantioenriched carbanions obtained by asymmetric deprotonation. One retrosynthesis (see scheme, above) involves *N*-Boc pyrrolidine (Boc = *tert*-butoxycarbonyl, Ar = aryl) and an organozinc intermediate, and the other (below) *O*-alkyl carbamates with organoboron intermediates.

Dioxo Complexes

Z. Gross* ——— 2737 – 2739

The Groves–Spiro Dioxomanganese(V) Story

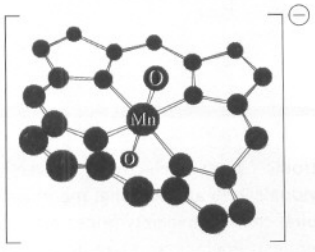

Double O agents: The first definitive spectroscopic evidence for *trans*-dioxomanganese(V) porphyrins (see picture) has been reported by Groves, Spiro, and co-workers. Their work extends the scope of oxo-coordination chemistry and opens the way for the exploration of reactivity patterns of *trans*-dioxo complexes of first-row transition-metal ions.

Contents

C–H Activation

M. Christmann* ——— **2740 – 2742**

Selective Oxidation of Aliphatic C–H Bonds in the Synthesis of Complex Molecules

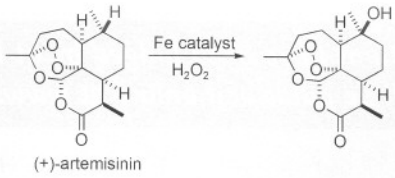

(+)-artemisinin

Tamed cat: Iron-catalyzed selective C–H oxidation reactions present new possibilities in the synthesis and modification of natural products. As a model reaction of a possible C–H oxidation as part of a total synthesis, the natural product (+)-artemisinin was converted into (+)-10β-hydroxyartemisinin in 34% yield (see scheme). The combination of nontoxic metal catalyst with H_2O_2 is an environmentally friendly process.

Minireviews

Membrane Proteins

H. Yin* ——— **2744 – 2752**

Exogenous Agents that Target Transmembrane Domains of Proteins

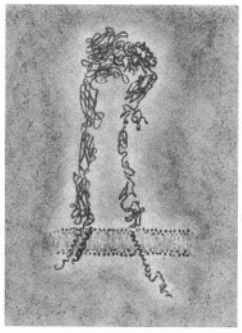

Over the limit: Despite accounting for about one third of all proteins encoded in the human genome, the functions and structures of the transmembrane domains of membrane proteins are poorly understood. Major advances have recently been made in the development of exogenous agents that can recognize these domains, which have laid the groundwork for targeting protein–protein interactions in the membrane bilayers (see picture).

Reviews

Liquid Crystals

J. W. Goodby,* I. M. Saez, S. J. Cowling, V. Görtz, M. Draper, A. W. Hall, S. Sia, G. Cosquer, S.-E. Lee, E. P. Raynes ——— **2754 – 2787**

Transmission and Amplification of Information and Properties in Nanostructured Liquid Crystals

Tune in your crystal set: Design of molecular shape, deformable molecular topologies, self-assembly, and self-organization combine together to yield super- and supramolecular liquid crystals (such as the nanomolecular "Boojum" shown in the picture) that are capable of exhibiting "superphases". Transmission and amplification of physical properties are often observed for such systems.

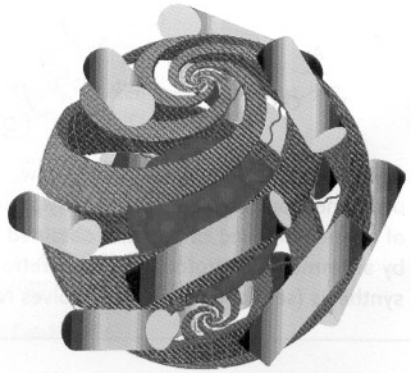

For the USA and Canada:
ANGEWANDTE CHEMIE International Edition (ISSN 1433-7851) is published weekly by Wiley-VCH, PO Box 191161, 69451 Weinheim, Germany. Air freight and mailing in the USA by Publications Expediting Inc., 200 Meacham Ave., Elmont, NY 11003. Periodicals postage paid at Jamaica, NY 11431. US POSTMASTER: send address changes to *Angewandte Chemie*, Wiley-VCH, 111 River Street, Hoboken, NJ 07030. Annual subscription price for institutions: US$ 7225/6568 (valid for print and electronic / print or electronic delivery); for individuals who are personal members of a national chemical society prices are available on request. Postage and handling charges included. All prices are subject to local VAT/sales tax.

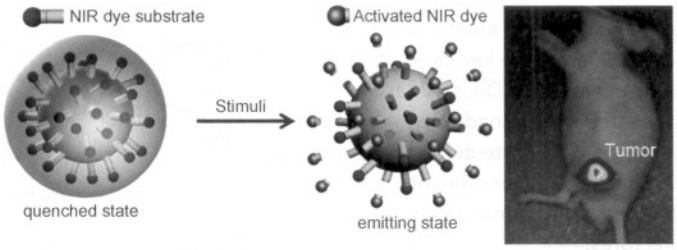

Nanodiagnosis: A matrix-metalloproteinase (MMP) sensitive gold-nanoparticle (AuNP) imaging probe quenches conjugated near-infrared (NIR) dyes with high efficiency and is specifically activated by the target MMPs (see picture, left). With this system, nanomolar amounts of protease can be detected—both in vitro and in vivo. Experiments disclose an apparent positive contrast in MMPs-positive tumor-bearing mice (right).

Gold Nanoprobes

S. Lee, E.-J. Cha, K. Park, S.-Y. Lee, J.-K. Hong, I.-C. Sun, S. Y. Kim, K. Choi, I. C. Kwon, K. Kim,* C.-H. Ahn* ——— **2804 – 2807**

A Near-Infrared-Fluorescence-Quenched Gold-Nanoparticle Imaging Probe for In Vivo Drug Screening and Protease Activity Determination

Beating the superbugs: Diversity-oriented synthesis using a solid-supported phosphonate unit to synthesize 242 drug-like compounds based on 18 natural-product-like scaffolds led to the discovery of gemmacin (see scheme). This new structural class of antibiotic is active towards methicillin-resistant *Staphylococcus aureus* (MRSA).

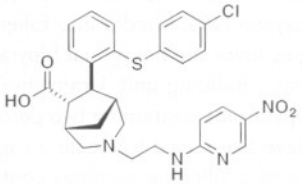

(–)-gemmacin

Combinatorial Chemistry

G. L. Thomas, R. J. Spandl, F. G. Glansdorp, M. Welch, A. Bender, J. Cockfield, J. A. Lindsay, C. Bryant, D. F. J. Brown, O. Loiseleur, H. Rudyk, M. Ladlow, D. R. Spring* — **2808 – 2812**

Anti-MRSA Agent Discovery Using Diversity-Oriented Synthesis

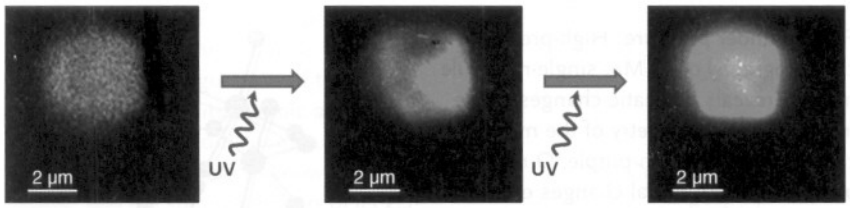

The right bright light: Silver-exchanged zeolite 3A crystals show remarkable luminescent properties. Upon irradiation with high-power UV light, a strong photoactivation process takes place which results in an emission increase of up to two orders of magnitude (see picture). The crystals of interest—or even small domains within one crystal—can be selectively activated by using a confocal microscope.

Silver in Zeolites

G. De Cremer, Y. Antoku, M. B. J. Roeffaers, M. Sliwa, J. Van Noyen, S. Smout, J. Hofkens, D. E. De Vos, B. F. Sels, T. Vosch* ——— **2813 – 2816**

Photoactivation of Silver-Exchanged Zeolite A

Variegated decomposers: The synthesis of the first mixed alkali metal borohydride, which contains lithium and potassium, is presented. $LiK(BH_4)_2$ (see picture; K crimson, Li yellow, B green, H gray) has a crystal structure similar to $LiBH_4$, and a thermal decomposition temperature between those of $LiBH_4$ and KBH_4. Using this route, the hydrogen desorption thermodynamics of complex hydrides can be easily tailored.

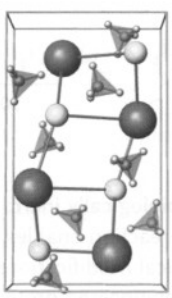

Hydrogen Storage

E. A. Nickels, M. O. Jones, W. I. F. David,* S. R. Johnson, R. L. Lowton, M. Sommariva, P. P. Edwards* ——— **2817 – 2819**

Tuning the Decomposition Temperature in Complex Hydrides: Synthesis of a Mixed Alkali Metal Borohydride

Contents

Organocatalysis

G. Evans, T. J. K. Gibbs, R. L. Jenkins, S. J. Coles, M. B. Hursthouse, J. A. Platts,* N. C. O. Tomkinson* ——— **2820 – 2823**

Kinetics of Iminium Ion Catalysis

Identifying the bottleneck: Kinetic and computational data for the key steps of the iminium ion catalyzed Diels–Alder reaction show that the cycloaddition (step II in scheme) is the rate-determining step of the catalytic cycle and provide a rationale for developing more-active catalyst architectures.

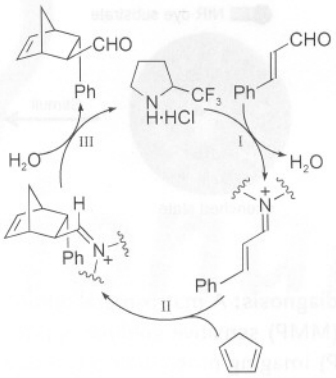

Inorganic Fullerene Structures

T. Z. Forbes, J. G. McAlpin, R. Murphy, P. C. Burns* ——— **2824 – 2827**

Metal–Oxygen Isopolyhedra Assembled into Fullerene Topologies

Conditions that permit the assembly of metal–oxygen isopolyhedra into fullerene topologies favor the hexagonal bipyramid as the basic building unit. Uranyl hexagonal bipyramids containing two peroxide edges have been used to create a cage cluster with a fullerene topology containing 50 polyhedra (see picture), as well as cage cluster of 40 polyhedra that contains topological squares, pentagons, and hexagons.

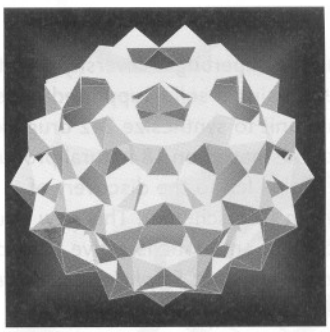

Pressure Effects

A. Prescimone, C. J. Milios, S. Moggach, J. E. Warren, A. R. Lennie, J. Sanchez-Benitez, K. Kamenev, R. Bircher, M. Murrie, S. Parsons,* E. K. Brechin* ——— **2828 – 2831**

$[Mn_6]$ under Pressure: A Combined Crystallographic and Magnetic Study

Folding under pressure: High-pressure crystallography of an Mn_6 single-molecule magnet reveals dramatic changes in the intramolecular geometry of the magnetic core (see picture; Mn purple, O red, N blue). These structural changes effect the magnetic properties of the molecule: the magnitude of the ferromagnetic exchange between the metals is decreased, and under extreme pressure switches to antiferromagnetic.

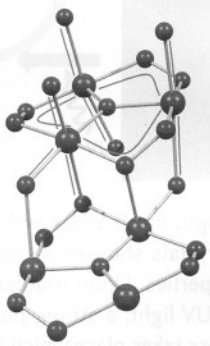

Bioorthogonal Chemistry

W. Song, Y. Wang, J. Qu, M. M. Madden, Q. Lin* ——— **2832 – 2835**

A Photoinducible 1,3-Dipolar Cycloaddition Reaction for Rapid, Selective Modification of Tetrazole-Containing Proteins

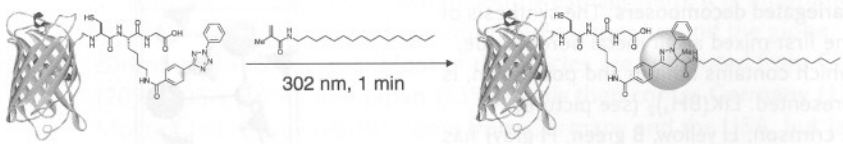

Reactive but biologically inert: The bioorthogonal title reaction enables highly specific chemical modifications, such as lipidation, of engineered proteins containing a diphenyltetrazole group (see scheme). The cycloaddition in biological media is extremely fast ($\leq$1 min) and tolerant of proteinaceous groups. Strongly fluorescent pyrazoline cycloadducts are generated with simple alkenes.

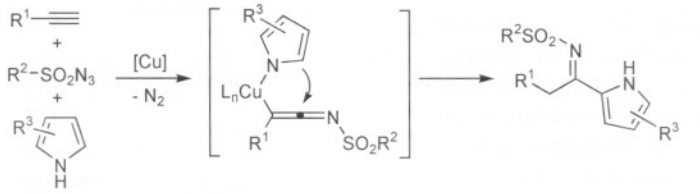

Making rings: A new Cu-catalyzed three-component coupling reaction between 1-alkynes, sulfonyl azides, and pyrrole derivatives has been developed for making 2-functionalized pyrrole rings (see scheme). This C–C bond formation offers high efficiency and selectivity, mild reaction conditions, and a wide substrate scope.

Pyrrole Functionalization

S. H. Cho, S. Chang* ____ **2836 – 2839**

Room Temperature Copper-Catalyzed 2-Functionalization of Pyrrole Rings by a Three-Component Coupling Reaction

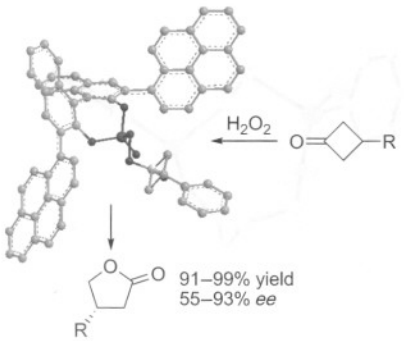

A catalytic amount of a chiral Brønsted acid with aqueous H_2O_2 as the oxidant is sufficient for the enantioselective Baeyer–Villiger oxidation of 3-substituted cyclobutanones to give the corresponding γ-lactones in excellent yields and up to 93% *ee*. The method employs benign aqueous H_2O_2 instead of stoichiometric amounts of a dangerous peracid.

Asymmetic Catalysis

S. Xu, Z. Wang, X. Zhang, X. Zhang, K. Ding* ____ **2840 – 2843**

Chiral Brønsted Acid Catalyzed Asymmetric Baeyer–Villiger Reaction of 3-Substituted Cyclobutanones by Using Aqueous H_2O_2

Synthesis in stereo: The first total synthesis of papuamide B, a cyclic peptide isolated from a marine sponge, has been achieved. The configuration of three stereogenic centers of its dienoic acid unit has been established by comparison to a series of stereoisomers of known configuration, and the stereochemistry of its 2,3-diaminobutanoic acid segment has been revised.

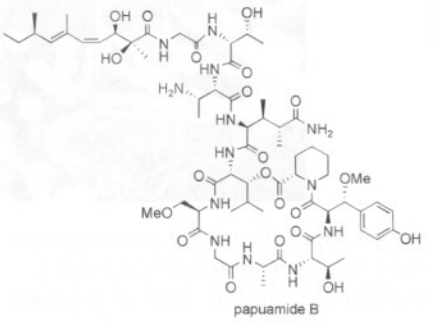

Natural Product Synthesis

W. Xie, D. Ding, W. Zi, G. Li, D. Ma* ____ **2844 – 2848**

Total Synthesis and Structure Assignment of Papuamide B, A Potent Marine Cyclodepsipeptide with Anti-HIV Properties

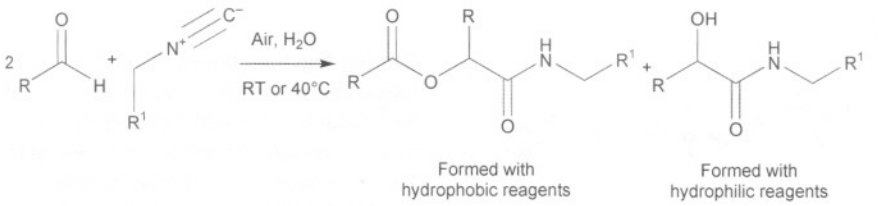

Wet, wet, wet: Hydrophobic aldehydes are cleanly oxidized upon stirring with water in air. Addition of hydrophobic isocyanides to aqueous suspensions of such aldehydes results in the formation of Passerini reaction products, with the aldehyde being the source of both carbonyl and ester functions. Partially water-soluble reagents reacted slower than water-insoluble ones. Isotope labeling studies show that water participates in these "on water" reactions.

Organic Synthesis

N. Shapiro, A. Vigalok* ____ **2849 – 2852**

Highly Efficient Organic Reactions "on Water", "in Water", and Both

Contents

Functional Foldamers

W. S. Horne, M. D. Boersma, M. A. Windsor, S. H. Gellman* ——— **2853 – 2856**

Sequence-Based Design of α/β-Peptide Foldamers That Mimic BH3 Domains

Into the fold: Foldamers have emerged as versatile scaffolds for the design of functional macromolecules. A straightforward design principle based on primary sequence can be used to convert an α-peptide ligand derived from a natural protein-binding domain into an α/β-peptide with comparable binding affinity for protein targets bound by the α-peptide (see scheme).

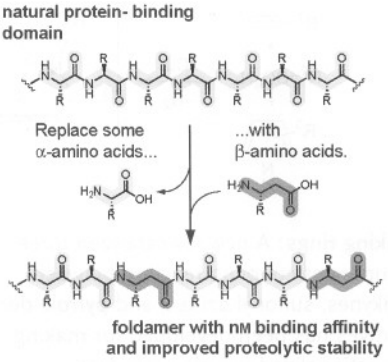

Organic P–Se Rings

G. Hua, Y. Li, A. M. Z. Slawin, J. D. Woollins* ——— **2857 – 2859**

Synthesis and Structure of Eight-, Nine-, and Ten-Membered Rings with P-Se-Se-P Linkages

Full circle: The reaction of [PhP(Se)(μ-Se)]$_2$ with alkyl or aryl diols affords five unusual P–Se heterocycles with eight-, nine-, and ten-membered rings containing P-Se-Se-P linkages. The structure of the ten-membered ring is shown.

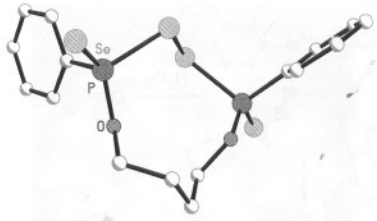

Biotin Structures

K. B. Joshi, S. Verma* ——— **2860 – 2863**

Ditryptophan Conjugation Triggers Conversion of Biotin Fibers into Soft Spherical Structures

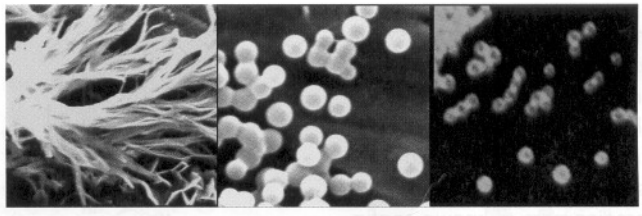

Trigger happy: Biotin and its methyl ester form long fibers in solution, which are transformed into soft spherical structures upon simple conjugation with ditryptophan dipeptide (see picture). Such morphogenesis is not achieved in a controlled fashion by other aromatic amino acids.

Electronic Structure

C. Mealli,* A. Ienco, A. Poduska, R. Hoffmann* ——— **2864 – 2868**

S_4^{2-} Rings, Disulfides, and Sulfides in Transition-Metal Complexes: The Subtle Interplay of Oxidation and Structure

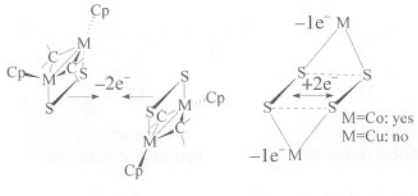

Coming together, breaking apart: A theoretical analysis of the oxidative coupling of two metal-coordinated disulfide species to a S_4^{2-} rectangle provides an opening to a reexamination of a number of compounds hitherto considered to be disulfide complexes. An electronic framework helps explain how the nature of the metal controls inner redox processes and the alternative stabilization of S_4^{2-} or $2\,S_2^{2-}$ (or S^{2-}) species (see scheme).

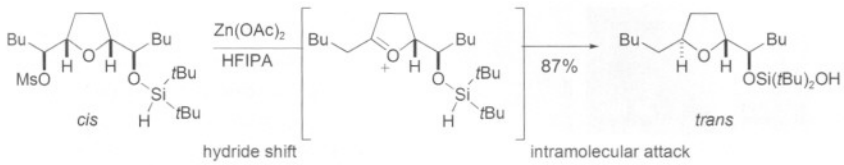

Switching sides: *cis* THF derivatives produced from the oxidative cyclization of dienes and diols can be transformed into the corresponding *trans* heterocycles through a 1,2-hydride shift and intramolecular trapping with a hydride nucleophile (see scheme). Moreover, organometallic compounds can be used to trap the oxonium ion generated in this way so that it is possible to introduce various groups at the C-2 position with control of stereochemistry.

Stereoselective Synthesis

T. J. Donohoe,* O. Williams, G. H. Churchill ——— **2869 – 2871**

Hydride Shift Generated Oxonium Ions: Evidence for Mechanism and Intramolecular Trapping Experiments to Form *trans* THF Derivatives

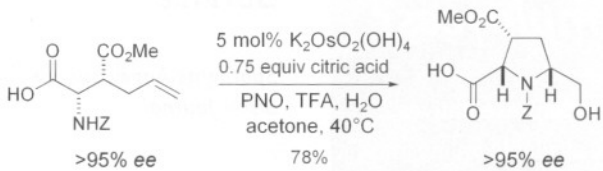

The PNOman can: The use of pyridine-*N*-oxide (PNO) transforms the catalytic oxidative cyclization to include the formation of pyrrolidines from N-Z-protected amino alcohols and amino acids (see scheme; Z = $PhCH_2OCO$). This new method expands the scope of the oxidative cyclization as illustrated with the synthesis of a range of di- and trisubstituted pyrrolidines with complete control of stereochemistry.

Oxidative cyclization

T. J. Donohoe,* K. M. P. Wheelhouse (née Gosby), P. J. Lindsay-Scott, P. A. Glossop, I. A. Nash, J. S. Parker ——— **2872 – 2875**

Pyridine-*N*-Oxide as a Mild Reoxidant Which Transforms Osmium-Catalyzed Oxidative Cyclization

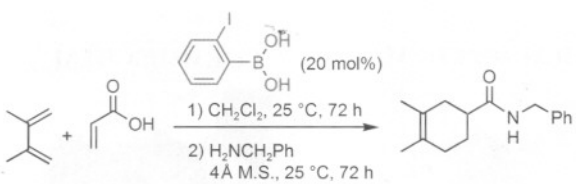

Taming carboxylic acids: *ortho*-Iodo- and *ortho*-bromophenylboronic acids are exceptional organocatalysts in atom-economical amidations between free carboxylic acids and amines, including functionalized ones, and can also provide LUMO-lowering activation in [4+2] cycloadditions of α,β-unsaturated carboxylic acids.

Organocatalysis

R. M. Al-Zoubi, O. Marion, D. G. Hall* ——— **2876 – 2879**

Direct and Waste-Free Amidations and Cycloadditions by Organocatalytic Activation of Carboxylic Acids at Room Temperature

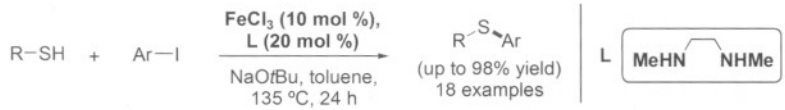

Strike while the iron is hot: An efficient iron-catalyzed protocol for the S-arylation of aromatic and heteroaromatic thiol derivatives has been developed, which involves an inexpensive catalyst system formed by combining $FeCl_3$ and *N*,*N*′-dimethylethylenediamine at 135 °C. This method avoids the use of expensive and/or air-sensitive ligands and provides in most cases the desired sulfide in high yields.

Cross-Coupling Reactions

A. Correa, M. Carril, C. Bolm* ——— **2880 – 2883**

Iron-Catalyzed S-Arylation of Thiols with Aryl Iodides

Contents

Shape effects

R. Si, M. Flytzani-Stephanopoulos* ——— 2884 – 2887

Shape and Crystal-Plane Effects of Nanoscale Ceria on the Activity of Au-CeO_2 Catalysts for the Water–Gas Shift Reaction

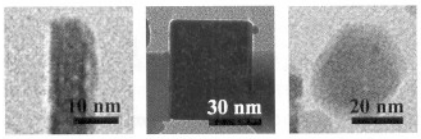

A two-step synthesis method is used to prepare gold-on-ceria nanorods, nanocubes, and nanopolyhedra (see picture), and a strong shape-effect of CeO_2 on the water–gas shift reaction activity of the catalysts is identified. Gold on the (110) facets of ceria nanorods shows the highest activity.

Supporting information is available on www.angewandte.org (see article for access details).

A video clip is available as Supporting Information on www.angewandte.org (see article for access details).

Service

Spotlights Angewandte's Sister Journals ——— 2724 – 2725

Keywords ——— 2888

Authors ——— 2889

Preview ——— 2891

Hydrogels

W. Deng, D. H. Yamaguchi, D. Y. Takashima, A. Harada*

Construction of Chemical-Responsive Supramolecular Hydrogels from Guest-Modified Cyclodextrins

Chem. Asian J.
DOI: **10.1002/asia.200700378**

Gelling together: Supramolecular hydrogels can be prepared from guest-modified cyclodextrins (CDs) by a method based on the host–guest and hydrogen-bonding interactions of CDs. These hydrogels display excellent chemical-responsive properties, and reversible gel-to-sol and sol-to-gel transitions occur upon the alternate addition of methyl orange and α-CD.

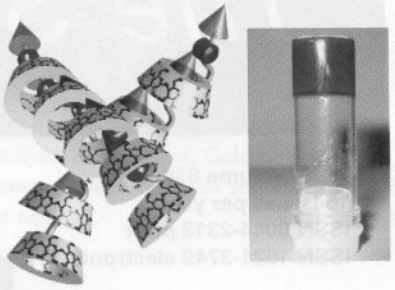

Site-Specific Labeling

S. Chattopadhaya, F. B. Abu Bakar, R. Srinivasan, S. Q. Yao*

In Vivo Imaging of a Bacterial Cell Division Protein Using a Protease-Assisted Small-Molecule Labeling Approach

ChemBioChem
DOI: **10.1002/cbic.200700647**

Announce on entry: We present a method for the site-specific labeling of target proteins using a set of cell permeable small-molecule probes. The tobacco etch virus (TEV) NIa protease, was used to generate target proteins with an N-terminal cysteine residue, which was subsequently labeled with thioester probe(s) in a site-specific and covalent manner. Furthermore, we demonstrate the utility of this approach for the study of FtsZ, an important bacterial cell-division protein (see figure).

Ionic Liquids

T. Köddermann, D. Paschek,* R. Ludwig*

Ionic Liquids: Dissecting the Enthalpies of Vaporization

ChemPhysChem
DOI: **10.1002/cphc.200700814**

Green vapors: The low volatility and the corresponding high heats of vaporisation make ionic liquids attractive as "green" solvents. Molecular dynamics simulations are able to reproduce thermodynamic properties of these new materials and can explain their origin on the basis of molecular interactions.

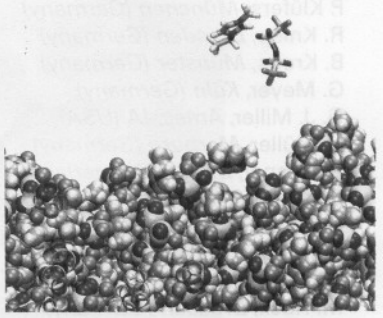

Enzyme Inhibitors

A. Agrawal, D. Romero-Perez, J. A. Jacobsen, F. J. Villarreal, S. M. Cohen*

Zinc-Binding Groups Modulate Selective Inhibition of MMPs

ChemMedChem
DOI: **10.1002/cmdc.200700290**

Improving MMP inhibition. Matrix metalloproteinases (MMPs) are a family of zinc-dependent endopeptidases. The zinc-binding group (ZBG) of matrix metalloproteinase inhibitors (MMPi) is shown to be effective in obtaining isoform selectivity. This suggests a novel route to obtaining targeted MMPi, which elicit specificity through both the ZBG and the peptidomimetic backbone.

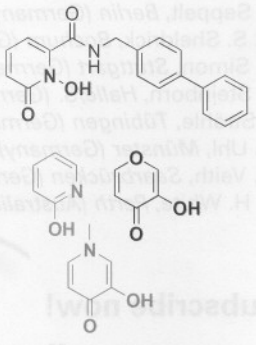

The hydrothermal synthesis and characterization (X-ray diffraction, IR, multinuclear NMR spectroscopy, electrochemistry) of the high-valent ruthenium-containing heteropolytungstate $[\{PW_{11}O_{39}\}_2\{(HO)Ru–O–Ru(OH)\}]^{10-}$ are reported. This complex can be obtained by the association of two $[PW_{11}O_{39}]^{7-}$ subunits linked by a $\{Ru^{IV}–O–Ru^{IV}\}$ diamagnetic core. Electrochemistry shows that it can be reversibly oxidized (one-electron process) or reduced (two-electron process).

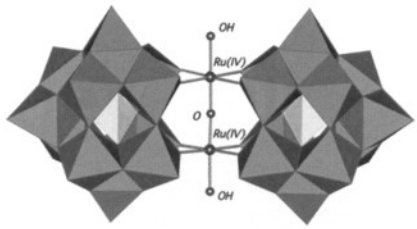

Ru-Containing Polyoxometalates

S.-W. Chen, R. Villanneau, Y. Li, L.-M. Chamoreau, K. Boubekeur, R. Thouvenot, P. Gouzerh, A. Proust*

Hydrothermal Synthesis and Structural Characterization of the High-Valent Ruthenium-Containing Polyoxoanion $[\{PW_{11}O_{39}\}_2\{(HO)Ru^{IV}–O–Ru^{IV}(OH)\}]^{10-}$

Eur. J. Inorg. Chem.
DOI: **10.1002/ejic.200701359**

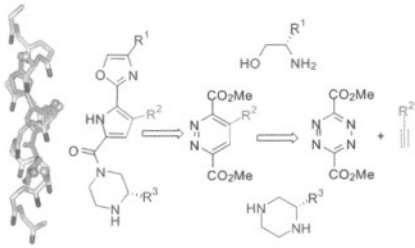

The design and synthesis of nonpeptidic α-helix mimetics based on a tricyclic oxazole–pyrrole–piperazine scaffold is described. The scaffolds present both a hydrophobic surface for recognition and a hydrophilic edge that is rich in hydrogen-bond donors and acceptors.

α-Helix Mimetics

L. Moisan, S. Odermatt, N. Gombosuren, A. Carella, J. Rebek Jr.*

Synthesis of an Oxazole–Pyrrole–Piperazine Scaffold as an α-Helix Mimetic

Eur. J. Org. Chem.
DOI: **10.1002/ejoc.200701164**

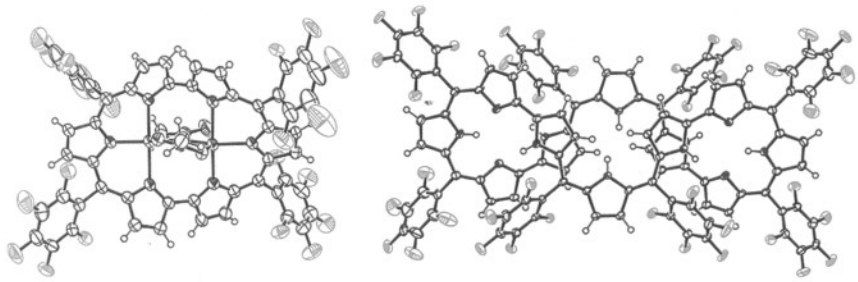

Aromatic switching has been demonstrated in both the absence and presence of a metal cation (i.e., zinc(II)) in the case of a *meso*-substituted rubyrin-type hexapyrrolic expanded porphyrin. This same system acts as an anion-binding agent in methanol solution, whereas the synthetic procedure used to prepare the parent compound, involving an oxidative coupling reaction of a *meso*-pentafluorophenyl substituted tripyrrane allows isolation of rubyrin-type expanded porphyrins.

Porphyrinoids

S. Shimizu, W.-S. Cho, J. L. Sessler,* H. Shinokubo, A. Osuka*

meso-Aryl Substituted Rubyrin and Its Higher Homologues: Structural Characterization and Chemical Properties

Chem. Eur. J.
DOI: **10.1002/chem.200701909**

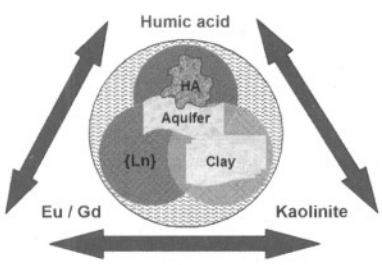

Heavy metal and rock: Humic acid (HA) in natural clays can play an important role in the (im)mobilization (complexation) of toxic metal ions such as radionuclides in the deep geological disposal of high-level radioactive waste. To better understand the influencing factors, the sorption behavior of Eu^{3+} and Gd^{3+} ions, as homologues of the actinides Am and Cm, was studied under various conditions.

Environmental Chemistry

R. Kautenburger,* H. P. Beck

Waste Disposal in Clay Formations: Influence of Humic Acid on the Migration of Heavy-Metal Pollutants

ChemSusChem
DOI: **10.1002/cssc.200800014**